

Origin of the codopant-induced enhancement of ferromagnetism in (Zn,Mn)O: Density functional calculations

Y. Zhu,^{1,2} J. X. Cao,² Z. Q. Yang,¹ and R. Q. Wu^{2,*}¹Surface Physics Laboratory (National Key Laboratory), Fudan University, Shanghai 200433, China²Department of Physics and Astronomy, University of California, Irvine, California 92697-4575, USA

(Received 9 January 2009; published 26 February 2009)

Using the density functional calculations, we elucidate the mechanism of codopant induced enhancement of ferromagnetism of (Zn,Mn)O. Li and Cu atoms tend to segregate toward Mn atoms and strongly promote the ferromagnetic coupling via either Ruderman-Kittel-Kasuya-Yosida or superexchange interaction. The hole states introduced by either Li or Cu are rather delocalized and they are efficient in mediating magnetic ordering. These findings shed light for the design of dilute magnetic semiconductors with codopants for spintronic applications.

DOI: [10.1103/PhysRevB.79.085206](https://doi.org/10.1103/PhysRevB.79.085206)

PACS number(s): 73.20.At, 73.61.Ey, 71.15.Nc

I. INTRODUCTION

ZnO is a wide-gap (3.4 eV) semiconductor with a large excitonic binding energy (60 meV) and hence is a promising multifunctional material for wide applications including in spintronic devices that operate with both charge and spin of electrons.¹ Nevertheless, it is still a major challenge nowadays to find effective means that may lead to substantial increase in the Curie temperature of ZnO-based dilute magnetic semiconductors (DMS). Experimental results for (Zn,Mn)O and (Zn,Co)O are rather inconsistent and the ferromagnetism observed at elevated temperatures is most likely associated with the presence of defects or precipitations in these materials.²⁻⁶ The Zener model description apparently breaks down for these systems⁷ since Mn is an isovalent substituent to Zn in the bulk wurtzite ZnO and hence the carrier density is extremely low in the perfect (Zn,Mn)O lattice. It is critical to establish reliable theoretical guidance for the search as design of functional ZnO-based DMS. Extensive first-principles calculations indicate that Mn²⁺ magnetic ions prefer antiferromagnetic (AFM) ordering because of the superexchange interaction.⁸⁻¹³ Nonetheless, the magnetic ground state can be altered by introducing itinerant carriers through lattice deficiencies or codopants.⁸ Interestingly, the presence of Li, Cu, and Al along with magnetic ions was found to be able to significantly promote the ferromagnetic (FM) ordering in (Zn,Co)O or (Zn,Mn)O.¹⁴⁻¹⁸ Although in principle this can be correlated with the mediation effect of nonlocal carriers, the fundamental mechanism behind the contributions of codopants toward the magnetic ordering of ZnO-based DMS is far from clearly understood.¹⁰

This paper focuses on revealing the mechanism of codopant induced enhancement of ferromagnetism by means of systematic density functional calculations in (Zn,Mn+X)O, with X=Li, Mg, Cu, Ga. These codopants are comparable in size to Zn and hence have good solubility into ZnO. In addition, they represent four distinctive effects to the magnetic ordering of (Zn, Mn)O: Li introduces one *s*-type hole; Cu brings in one *d*-type hole; Mg has no *d* electrons; and Ga has one extra electron. Dramatically, we found that both Li and Cu tend to segregate to region near Mn atoms and strongly promote the ferromagnetic coupling between

Mn spins. These findings and their fundamental origin should be important for successful fabrication of excellent (Zn,Mn)O DMS for room-temperature spintronic applications. Detailed discussions are given in Sec. III, right after a brief description of method and computational aspects below.

II. METHOD AND COMPUTATIONAL DETAILS

The present calculations were carried out by using the *ab initio* pseudopotential plane-wave method as implemented in the Vienna *ab initio* simulation package (VASP) package.¹⁹ We adopted the generalized gradient approximation (GGA) (Ref. 20) for the description of the exchange-correlation interaction and we also examined the strong correlation effect with the LSDA+*U* approach²¹ for several systems. An energy cutoff of 360 eV was employed for the expansion of wave functions. Test calculations with $E_{\text{cut}}=450$ eV and 550 eV indicate that the strength of Mn-Mn exchange interaction, measured as the difference between the total energies of the AFM and FM states, $\Delta E_{\text{AFM-FM}}=E_{\text{AFM}}-E_{\text{FM}}$, converges to better than 2 meV. We optimized lattice sizes and atomic positions through GGA calculations with a criterion that requires the calculated forces less than 10^{-2} eV/Å.

To permit appropriate exploration of different atomic configurations with three impurity atoms, we used a large $3 \times 3 \times 3$ wurtzite supercell as shown in Figs. 1(a) and 1(b). This cell contains 108 atoms, and the substitution of two Mn atoms corresponds to a Mn concentration of 3.7%, a ratio which corresponds to most experimental observations for (Zn,Mn)O.^{2,5} To retain sufficient Mn-Mn exchange interaction yet without scarifying generality, we considered two geometries with the first Mn atom being fixed at the site-0 and the second Mn atom being placed either at the site-2 or site-3. For simplicity of discussions below, we denote them as the 02 and 03 configurations, respectively. We also use abbreviations for configurations with codopants. For example, 03Cu_1 stands for the case shown in Fig. 1(a) that has Cu substituting Zn at the site-1 in the 03 configuration.

III. RESULTS AND DISCUSSIONS

For (Zn,Mn)O, our GGA calculations indicate that the 02 structure is lower in total energy by 88 meV/cell than the 03

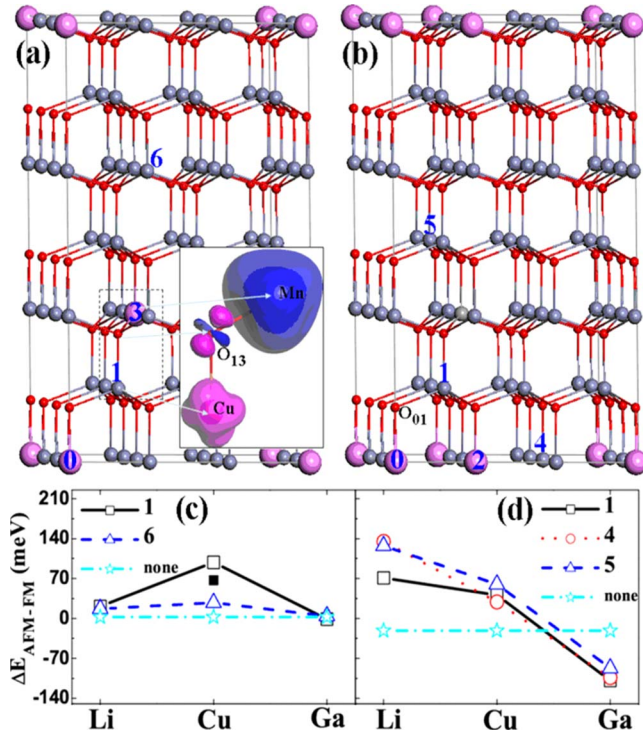


FIG. 1. (Color online) The unit cell for the (a) 03 and (b) 02 configurations in the ball-stick format. Small light gray and red (dark) balls are for Zn and O atoms while large pink (gray) balls are for Mn. The inset in panel (a) shows the spin density around Cu and Mn with blue (dark) isosurfaces giving positive spin density whereas the pink (light gray) isosurfaces giving negative spin density. Panels (c) and (d) provide the exchange energies for the 03 and 02 configurations with and without the presence of codopants. The filled box in panel (c) is the LDA+ U result for the 03Cu_1 configuration.

configuration. Due to the large separation, $d_{\text{Mn-Mn}}=6.21 \text{ \AA}$, the Mn-Mn exchange interaction in the 03 configuration is negligible as reflected in the small energy difference, $\Delta E_{\text{AFM-FM}}=2 \text{ meV/cell}$. In the 02 configuration, the two Mn atoms couple through an oxygen atom underneath and therefore the superexchange mechanism plays a major role. As a result, the AFM state is more preferential with a sizable energy difference, $\Delta E_{\text{AFM-FM}}=-22 \text{ meV/cell}$. These results are close to those of previous density functional calculations performed with a $2 \times 2 \times 2$ wurtzite supercell.^{10,12,13} With the presence of codopants, we found that the substitution of Mg for Zn does not change $\Delta E_{\text{AFM-FM}}$ much, within a range of 2 meV. This demonstrates that the d states of Zn are insignificant for the magnetic properties of (Zn,Mn)O.

Interestingly, Li and Cu strongly promote the ferromagnetic ordering in both 02 and 03 configurations, as displayed in Figs. 1(c) and 1(d). In particular, the value of $\Delta E_{\text{AFM-FM}}$ increases to as much as 70–140 meV when Li is introduced into the 02 configuration. (Zn,Mn+Cu)O also has a stable FM ground state in both 02 and 03 geometries with high values of $\Delta E_{\text{AFM-FM}}$ up to 80 meV. Such large exchange energies certainly lead to drastic enhancement in the Curie temperature of (Zn,Mn)O, needed for practical applications. We also conducted LDA+ U calculations, using parameters U

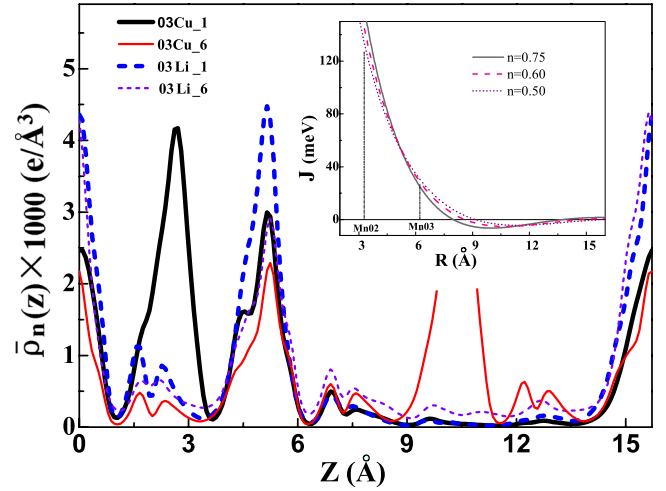


FIG. 2. (Color online) Planar averaged hole density distributions for the 03 configuration along the z axis. The inset shows the strength of the RKKY exchange interaction for different hole densities in unit of 10^{-3} e/\AA^3 .

$=4.5 \text{ eV}$ and $J=0.8 \text{ eV}$ for the d bands of Zn and Cu, and found that the value of $\Delta E_{\text{AFM-FM}}$ is somewhat reduced but still remains substantial. For example, $\Delta E_{\text{AFM-FM}}$ obtained through LDA+ U calculations is 70 meV for the 03Cu_1 geometry, as indicated by the filled box in Fig. 1(c). Since the LDA+ U approach sets an upper limit for the correlation effect, the predicted strong enhancement of ferromagnetism induced by Li and Cu is trustworthy.

It is reasonable to depict that Li donates its $2s$ electron to an adjacent O, and meanwhile introduces a hole into (Zn,Mn)O. Since this hole is s type and delocalized, the primary mechanism of the enhanced ferromagnetic ordering in (Zn,Mn+Li)O should be via the Ruderman-Kittel-Kasuya-Yosida (RKKY) interaction. In Fig. 2, one can find that the hole from Li mainly distributes around Mn and in the region between them. If we use the average hole density $\bar{\rho} = 0.50-0.75 \times 10^{-3} \text{ e/\AA}^3$ and plot the value of J_{RKKY} as a function of $d_{\text{Mn-Mn}}$, it is clear that J_{RKKY} for the 02 configuration is much larger than that for the 03 configuration as shown in the inserted part in Fig. 2. Clearly, different Mn-Mn distances in the 02 and 03 configurations instigate the drastic difference of the effect of Li toward mediating their magnetization in Figs. 1(c) and 1(d). Another remarkable finding here is that the density of hole in the region between two Mn atoms is almost independent of the location of the Li codopant, even when it is placed remotely at the site-6. This indicates the effectiveness of using Li for the curie temperature enhancement of (Zn,Mn)O. The delocalization nature of holes provided by Li and Cu is also beneficial for mediating percolation among spin-polarized regions in the ZnO lattice, another important factor for establishment of long-range magnetic ordering in DMS as addressed by Bergqvist *et al.*²² Furthermore, the RKKY mechanism is more appropriate than the double exchange one used by Sluiter *et al.*¹⁰ for the interpretation of Li-induced enhancement of magnetic coupling in ZnO-based DMS.

In principle, the hole provided by the Cu codopant is d like and is spin polarized since Cu carries a local magnetic

moment $M_{\text{Cu}} = \mu_B$ in $(\text{Zn,Cu})\text{O}$.²³ This triggers the superexchange interaction between Cu and Mn through O atoms. As a result, the Cu magnetic moment tends to be antiparallel to those of Mn at both ends in the 03Cu_1 configurations, as seen from the isosurfaces of spin density in the inset in Fig. 1(a). As a result, the magnetic moments of Mn ought to align parallel to each other, leading to a strong FM state as shown in Figs. 1(c). If Mn moments are set to be antiparallel as in the AFM state, Cu holds its local magnetic moment of μ_B through the LDA+ U calculations, but loses its magnetization in the GGA calculations. This mechanism also applies to the 02Cu_1 configuration, as seen in Fig. 1(d). In addition the RKKY interaction and the superexchange across the Mn-O-Mn bonds also play a role in the 02 configurations. In particular, we found that the hole brought in by Cu still possesses significant itinerant feature, as manifested by the substantial magnitude of $\bar{\rho}$ between the two Mn atoms in the 03Cu_6 configuration in Fig. 2. This feature leads to an insensitivity of $\Delta E_{\text{AFM-FM}}$ to the location of Cu as shown in Fig. 1(d) for 02Cu_ i ($i=1,4,5$) configurations.

It is worth of mentioning that Copal *et al.*¹² found that $(\text{Zn,Mn+Cu})\text{O}$ is AFM in their calculations with a $2 \times 2 \times 2$ supercell. However, these results should be viewed cautiously since the cell gives an unrealistic high doping concentration, 18.75%. We also performed calculations using the $2 \times 2 \times 2$ supercell, and found that the AFM alignment is more preferred in both cases, with $\Delta E_{\text{AFM-FM}} = -5 \sim -40$ meV, depending on the relaxation and inclusion of the U term. Interestingly, Cu atom shifts toward Mn atoms with $d_{\text{Cu-Mn}} = 2.59$ Å, a value that is much smaller than the nearest Zn-Zn distance in the bulk wurtzite ZnO, 3.24 Å. This drastic local distortion disappeared ($d_{\text{Cu-Mn}} = 3.20$ Å) when we adopted the $3 \times 3 \times 3$ supercell, which corresponds to practical doping concentration, 5.6%. Therefore, the use of small cells leads to unrealistic predictions for properties of DMS, especially with the presence of codopants.

Doping of Mn into the ZnO lattice does not produce free carriers and hence the holes brought in by Li and Cu codopants are crucial for the coupling of magnetic moments of Mn^{2+} . To demonstrate this, curves of partial density of states (DOS) of Mn in the majority-spin channel are plotted in Fig. 3(a) for four different configurations. It is clear that both Li and Cu brings in holes within 0~0.3 eV. For, $(\text{Zn,Mn+Li})\text{O}$ the hole state is delocalized but mainly distributes in the O sublattice. The $(\text{Zn,Mn+Li})\text{O}$ is half-metallic and hence the holes are 100% spin polarized. Compared to results for $(\text{Zn,Mn})\text{O}$, the Mn d band shows a rigid shift and the Mn magnetic moments are reduced by $0.1-0.15\mu_B$ to $4.85-4.9\mu_B$ per Mn. In addition, the Mn d band in the 02 configurations is somewhat broader than that in the 03 configurations because of stronger Mn-Mn hybridization.

In Figs. 3(b) and 3(c), we plotted the DOS of Cu d bands and O p bands in the 02Cu_1 and 03Cu_1 configurations to elucidate the Mn-Cu and Mn-O hybridizations. In the spin-down channel, the Mn states lie well above the Fermi level and therefore the Cu d states mainly interact with O p states in the occupied regime. In the spin-up channel, the mixing among Mn, Cu, and O states are obvious from the numerous resonant peaks around the Fermi level. The Cu induced hole

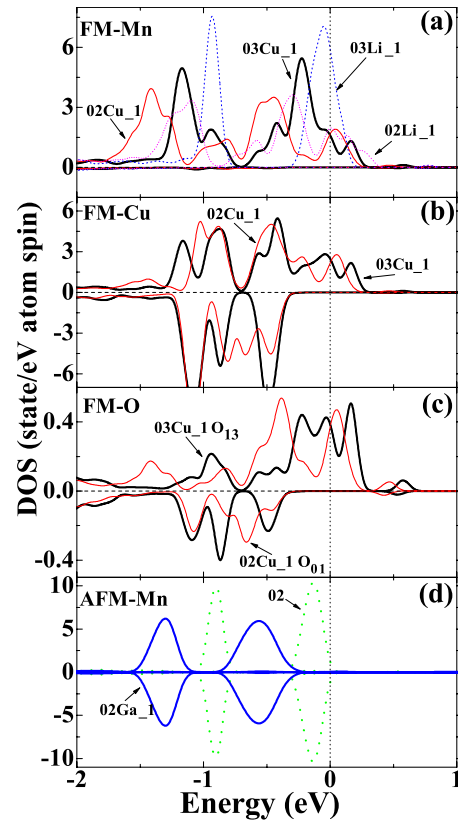


FIG. 3. (Color online) The projected density of states (DOS) of Mn, Cu, and O atoms in selected configurations. Zero energy indicates the position of the Fermi level. Positive and negative values of DOS are for the spin-up and spin-down channels, respectively.

states have positive spin polarization in the entire space. Nevertheless, due to the complete occupancy of the Cu spin-down d states, the net magnetic moment on Cu is negative.

Now we answer a question what happens if the codopants bring in excessive electrons. Based on the band model, it was argued that the AFM state prevails in the n -type $(\text{Zn,Mn})\text{O}$. However, Sluiter *et al.*¹⁰ found that both hole and electron promote FM ordering in this material, based on the density functional calculations in the $2 \times 2 \times 2$ unit cell. Ferromagnetism has also been observed in n -type $(\text{Zn,Mn})\text{O}$, with free electrons from Al codopants and interstitial Zn. Here we found that, regardless its location, Ga has negligible effect on the magnetic ordering of the 03 configuration while further reinforces the AFM ordering in the 02 configuration. Therefore, we may attribute the observed ferromagnetism in $(\text{Zn,Mn+Al})\text{O}$ to extrinsic effects such as the precipitation of metal atoms or local compounds. From the curves of density of states in Fig. 3(d), we found that the additional free electron fills the conduction band of ZnO since the spin-down states of Mn are higher in energy. Therefore electrons from Ga take positions away from the region around Mn, mostly in the O sublattice. As a result of the rehybridization and charge transfer, the Mn d states shift downward in energy and the bands are somewhat broadened with the presence of Ga. These indicate the enhanced superexchange interaction between Mn ions in the environment that has excessive electrons.

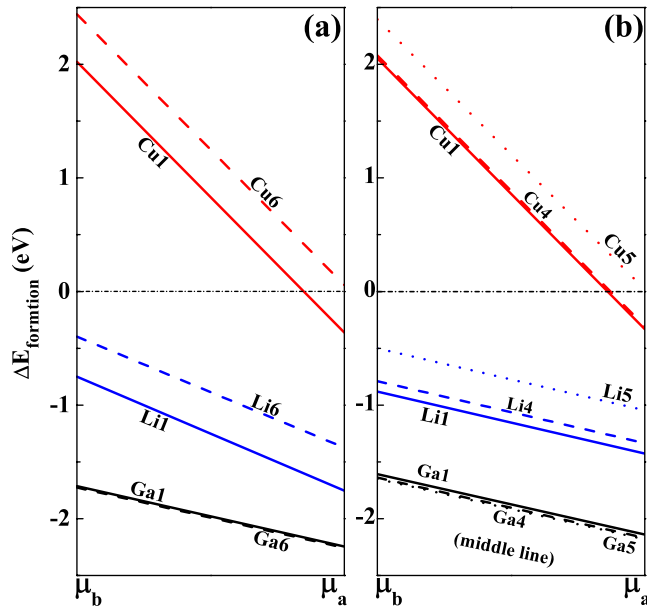


FIG. 4. (Color online) (a) Formation energies for structures with either Li, Cu, or Ga substituting Zn at different sites as a function of chemical potentials from μ_b (bulk) and μ_a (atom). Panels (a) and (b) are for the 03 and 02 configurations, respectively.

To investigate the segregation behavior of different codopants in (Zn,Mn)O, we plotted the formation energies that is defined as

$$E_{\text{Formation}} = (E_{(\text{Zn,Mn}+X)\text{O}} - \mu_X) - (E_{\text{ZnMnO}} - \mu_{\text{Zn}}) \quad (1)$$

using the chemical potentials, μ_X , of Ga, Cu, and Li in both bulk or gas phases. μ_{Zn} represents the chemical potentials of Zn in its bulk and gas phases, respectively. Such a definition covers two extremes, using either bulks or individual atoms as the reservoirs. We found it is rather difficult to have Cu segregated into (Zn,Mn)O from its bulk phase. As displayed in Fig. 4, the formation energy stays in the positive side for Cu taking either site 1 or 6, regardless the use of reference chemical potentials. The formation energy is negative only

under the conditions that Cu is placed at the site-1 and the gas phase Cu is used as the reservoir. In contrast, the formation energy of Li is always below zero in Fig. 4, with the site-1 the most preferential one. It means that Li can easily penetrate into (Zn, Mn)O, especially to the region near the Mn atoms. In conjunction with the substantial enhancement of ferromagnetism induced by Li in almost any position, one can see that the incorporation of Li is probably the best strategy for the increase in the Curie temperature of (Zn,Mn)O. Ga also can easily penetrate into (Zn, Mn)O in all sites especially into remote site as shown in Fig. 4 but it promote AFM ordering, not beneficial for practical usage.

IV. CONCLUSION

In summary, we systematically investigated the effect of codopants on the exchange interaction in (Zn,Mn)O. It is important that Li and Cu strongly promote the ferromagnetic ordering via the RKKY, superexchange, and double exchange mechanisms. From aspects of both formation energy and magnetic effect, Li might be the best codopant for the fabrication of functional ZnO-based magnetic semiconductors. Although we addressed only the codoping effect on the exchange interaction between two Mn atoms, the delocalized holes should also be beneficial for the percolation of magnetized regions throughout the lattice. These important findings shed lights for the design of spintronic materials that are crucial for technological innovations.

ACKNOWLEDGMENTS

Work is supported by U.S. DOE (Grant No. DEFG02-05ER46237). Z.Q.Y. and Y.Z. also acknowledge support from the National Science Foundation of China (Grant No. 10674027), the Grant Foundation of Shanghai Science Technology (Grant No. 05DJ14003) and 973 Project (Grant No.2006CB921300), and the China Scholarship Council. We are grateful to X. Wang and L. Ye in Fudan University for very helpful discussion. Calculations were performed on computers at NERSC and Fudan High-End Computing Center.

*wur@uci.edu

¹S. J. Pearton, C. R. Abernathy, M. E. Overberg, G. T. Thaler, D. P. Norton, N. Theodoropoulou, A. F. Hebard, Y. D. Park, F. Ren, J. Kim, and L. A. Boatner, *J. Appl. Phys.* **93**, 1 (2003).
²T. Fukumura, Zhengwu Jin, M. Kawasaki, T. Shono, T. Hasegawa, S. Koshihara, and H. Koinuma, *Appl. Phys. Lett.* **78**, 958 (2001).
³K. Ueda, H. Tubata, and T. Kawai, *Appl. Phys. Lett.* **79**, 988 (2001).
⁴W. Prellier, A. Fouchet, B. Mercey, C. Simon, and B. Raveau, *Appl. Phys. Lett.* **82**, 3490 (2003).
⁵P. Sharma, A. Gupta, K. V. Rao, F. J. Owens, R. Sharma, R. Ahuja, J. M. O. Guillen, B. Johansson, and G. A. Gehring, *Nat. Mater.* **2**, 673 (2003).

⁶C. Liu, F. Yun, and H. Morkoç, *J. Mater. Sci. Mater. Electron.* **16**, 555 (2005).
⁷T. Dietl, H. Ohno, F. Matsukura, J. Cibert, and D. Ferrand, *Science* **287**, 1019 (2000).
⁸K. Sato and H. Katayama-Yoshida, *Semicond. Sci. Technol.* **17**, 367 (2002).
⁹M. S. Park and B. I. Min, *Phys. Rev. B* **68**, 224436 (2003).
¹⁰M. H. F. Sluiter, Y. Kawazoe, P. Sharma, A. Inoue, A. R. Raju, C. Rout, and U. V. Waghmare, *Phys. Rev. Lett.* **94**, 187204 (2005).
¹¹T. Chanier, M. Sargolzaei, I. Opahle, R. Hayn, and K. Koepf, *Phys. Rev. B* **73**, 134418 (2006).
¹²P. Gopal and N. A. Spaldin, *Phys. Rev. B* **74**, 094418 (2006).
¹³A. Walsh, J. L. F. Da Silva, and S. H. Wei, *Phys. Rev. Lett.* **100**,

- 256401 (2008).
- ¹⁴H. T. Lin, T. S. Chin, and J. C. Shih, *Appl. Phys. Lett.* **85**, 621 (2004).
- ¹⁵X. C. Liu, E. W. Shi, Z. Z. Chen, H. W. Zhang, B. Xiao, and L. X. Song, *Appl. Phys. Lett.* **88**, 252503 (2006).
- ¹⁶O. D. Jayakumar, I. K. Gopalakrishnan, K. Shashikala, S. K. Kulshreshtha, and C. Sudakar, *Appl. Phys. Lett.* **89**, 202507 (2006).
- ¹⁷M. Venkatesan, P. Stamenov, L. S. Dorneles, R. D. Gunning, B. Bernoux, and J. M. D. Coey, *Appl. Phys. Lett.* **90**, 242508 (2007).
- ¹⁸Y. H. Lin, J. N. Cai, C. W. Nan, M. Kobayashi, and J. L. He, *J. Appl. Phys.* **99**, 056107 (2006).
- ¹⁹G. Kresse and D. Joubert, *Phys. Rev. B* **59**, 1758 (1999).
- ²⁰Y. Wang and J. P. Perdew, *Phys. Rev. B* **44**, 13298 (1991).
- ²¹V. Anisimov, F. Aryasetiawan, and A. Lichtenstein, *J. Phys.: Condens. Matter* **9**, 767 (1997).
- ²²L. Bergqvist, O. Eriksson, J. Kudrnovsky, V. Drchal, P. Korzhavyi, and I. Turek, *Phys. Rev. Lett.* **93**, 137202 (2004).
- ²³L. H. Ye, A. J. Freeman, and B. Delley, *Phys. Rev. B* **73**, 033203 (2006).